IOSR Journal of Mechanical and Civil Engineering (IOSR-JMCE)
e-ISSN: 2278-1684, p-ISSN: 2320-334X
PP 55-62
www.iosrjournals.org

Seismic Control of Benchmark Highway Bridge Installed with Friction Pendulum System

Suhasini N. Madhekar
Associate Professor, Applied Mechanics,
College of Engineering Pune, Pune 411005, India
suhasinimadhekar@gmail.com

***ABSTRACT*:** *Major earthquakes of the last few decades have generated a great deal of interest in structural control systems, to mitigate seismic hazards to lifeline structures - in particular, bridges. The vast destruction during earthquakes underscores the importance of finding more rational and substantiated solutions for protection of bridges. One of the most promising devices, considered as a structural control system, is seismic isolation. A benchmark problem on Highway Bridge has been developed to compare the performance and effectiveness of different control systems in protecting bridges from earthquakes. In the present study, response of the bridge, with sliding isolator is investigated with conventional Friction Pendulum System (FPS), under six earthquake ground motions. The problem is based on the highway over-crossing at Southern California, USA. It is concluded that with the installation of sliding isolators, the seismic response of the bridge under near-fault motions can be controlled significantly.*

***Keywords*:** *Benchmark Highway Bridge, Structural control, Seismic Isolation, Friction Pendulum System, Lead Rubber Bearing.*

1. Introduction

Recent devastating earthquakes have revealed that bridges are the most vulnerable components of transportation systems. Total collapse or severe damage of bridges is observed in Indian earthquakes, such as Latur(1993), Jabalpur (1997), Chamoli (1999), and the most recent, Bhuj (2001) earthquake. The Northridge earthquake (January 17, 1994) in the United States caused extensive damage and collapse of several conventionally designed highway bridges. Exactly one year later (January 17, 1995), a devastating earthquake struck the city of Kobe, Japan. This event was a massive disaster that overshadowed the Northridge earthquake. Collapse scenarios in the earthquakes involved severe column flexural and shear failures due to their nonlinear behaviour, and unseating at in-span and abutment bearings due to excessive displacements. Bridges are prone to large bearing displacements and deck accelerations, because of their low structural redundancy and small inherent damping. Disruption in the transportation network due to partial ortotal collapse of bridges after a major earthquake would seriously hamper the relief and rehabilitation operations.

Conventionally, safety of bridges is enhanced by making its members stronger and more ductile, so that they can withstand higher forces. The traditional method of providing for lateral load carrying capacity, allows the entire ground motion to be transmitted to the superstructure. From cost considerations, it is not feasible to design a bridge to resist the design earthquake elastically. Hence, the bridge absorbs energy through inelastic action, which inevitably damages structural and non-structural elements. Currently, bridges are designed to be sufficiently stiff, and it is a common practice to rely on inelastic yielding of structural components. However, this is not an efficient design practice, because after the structural components yield, their load carrying capacity is exhausted, and this makes the bridge vulnerable to the next set of dynamic loads. Strength based design philosophy is not suitable for lifeline structures like bridges. Furthermore, in a severe earthquake, the deformations may be well beyond the elastic limit and the loads are significantly greater than the design loads. This indicates that bridges designed with conventional methods are still vulnerable to strong earthquake motions.

The performance of bridges during earthquakes can be improved by introducing suitable energy dissipation mechanisms in the bridge system. Structural protective systems may be implemented in bridges to dissipate a large amount of energy, and mitigate the damaging effects of dynamic forces. Structural control may be utilized either to reduce the

amount of energy transferred into the bridge structure from the ground motion, or to absorb some of the earthquake energy after it has been transferred to the bridge. The seismic isolation bearings, which usually replace conventional bridge bearings, decouple the superstructure from piers and abutments during earthquakes. This significantly reduces the seismic forces induced in the bridge structure, and lowers the strength and ductility demands on the bridge. A benchmark problem for seismically excited highway bridges has been developed for response control of highway bridges(Agrawal et al., 2009). It provides a systematic and standardized means by which competing control strategies including devices, control algorithms and sensors, can be evaluated. The bridge model is based on the highway bridge in southern California, USA. The response of the bridge to six different real earthquake ground excitations is investigated using simplified lumped mass finite element model of the bridge. In phase I, eight control devices are located between the deck-end and abutments, and in phase II, two additional devices are provided at the center. The optimum device parameters are investigated to improve response of the bridge. The present study explores the use of sliding seismic isolator, namely, Friction Pendulum System (FPS). The effectiveness of FPS is explored in terms of reduction of the specified evaluation criteria. The focus of the study is on reducing the peak base shear, mid-span displacement and bearing displacement. The analytical simulation results demonstrate that FPS, under optimum parameters, is quite effective and can be practically implemented for the vibration control of bridges.

2. The Benchmark Highway Bridge

The bridge model used for the benchmark study is that of the 91/5 highway overcrossing in Southern California. Seismic design considerations were duly considered in the design of this bridge, as it is located very close to two major faults and its critical role as a principal overcrossing. The superstructure of the bridge consists of a two-span continuous, cast-in-situ pre-stressed concrete (PC) 3-cell box-girder and the substructure is in the form of PC outriggers. Each span of the bridge is 58.5m long, spanning a four-lane highway, with two skewed abutments. The deck is supported by a 31.4m long and 6.9m high PC outrigger, resting on pile foundation. In the actual bridge, four conventional elastomeric bearings are provided at each abutment and four passive fluid dampers are installed between each abutment and the deck-end. In the evaluation model, LRBs are used in place of the elastomeric bearings. The uncontrolled structure, used as a basis of comparison for the controlled system, corresponds to the model, isolated with four LRBs at each deck-end. Figure 1 shows the elevation and plan view of the bridge. Figure 2 shows typical location of control devices and accelerometers. Transverse (referred as *x*-direction) is the N-S and the longitudinal (referred as *y*-direction) is the E-W.

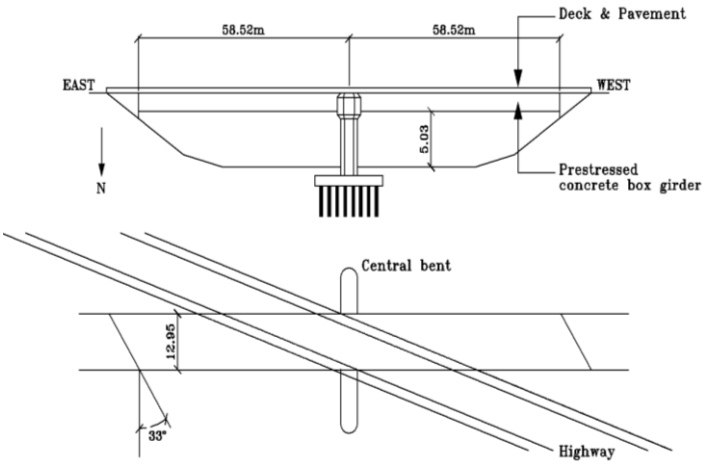

Fig. 1: Elevation and plan view

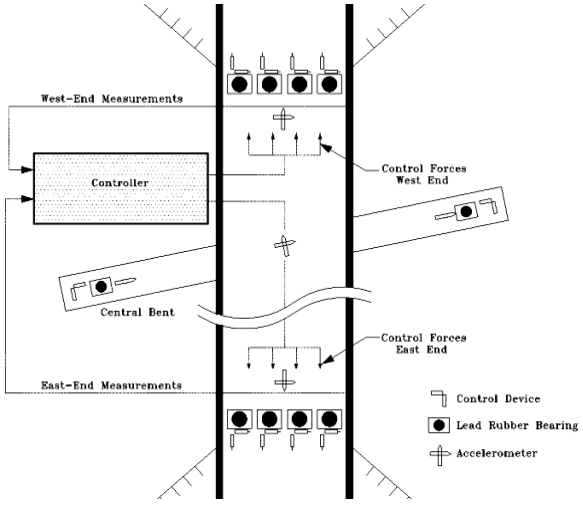

Fig.2: Location of devices and accelerometers

2.1Governing Equations of Motion

The governing equations of motion are obtained by considering equilibrium of forces at the location of each DOF during seismic excitations. Under strong earthquake excitations, highway bridges exhibit nonlinear hysteretic behavior caused by inelastic deformation of piers and soil-structure interaction. Hence, a nonlinear response-history analysis in time domain is employed. The nonlinear finite element model of the bridge is considered excited under two horizontal components of earthquake ground motion, applied along the two orthogonal directions. The responses in both directions are considered to be uncoupled and there is no interaction between frictional forces. The equations of motion of the evaluation model (1), (2) and (3) are expressed in the following matrix form,

$$[M]\{\ddot{u}(t)\} + [C]\{\dot{u}(t)\} + [K]\{u(t)\} + [b]\{F(t)\} \quad (1)$$

$$\{u(t)\} = \{x_1, x_2, x_3, \ldots, x_N, y_1, y_2, y_3, \ldots, y_N\}^T \quad (2)$$

$$\{\ddot{u}_g\} = \begin{Bmatrix} \ddot{x}_g \\ \ddot{y}_g \end{Bmatrix} \quad (3)$$

where [*M*], [*C*] and [*K*(*t*)] are the mass, damping and stiffness matrix, respectively of the bridge structure of the order *2N×2N*; $\{\ddot{u}(t)\}, \{\dot{u}(t)\}$ and $u(t)$ are structural acceleration, structural velocity and structural displacement vectors, respectively of size *N×1*; $\ddot{u}_g(t)$ is the vector of earthquake ground accelerations acting in two horizontal directions; $\ddot{x}_g$ and $\ddot{y}_g$ represent the earthquake ground accelerations (m/sec^2) in the transverse and longitudinal directions, respectively; x_i and y_i denote displacements of the i^{th} node of the bridge in transverse and longitudinal directions, respectively; $\{F(t)\}$ is the vector of control force inputs; $\{\eta\}$ is the influence coefficient vector; and {*b*} is the vector defining how the forces produced by the control devices enter the structure. The lumped mass matrix [*M*] has a diagonal form. The stiffness matrix [*K*(*t*)] is the combination of [K_L+ K_N(*t*)] where the K_L is the linear part of the stiffness matrix and K_N(*t*)is the nonlinear part. The global damping matrix, [*C*]is expressed as a combination of the distributed inherent damping in the structure and soil radiation damping. It is assumed that the properties of the system remain constant during the time-step of analysis.

2.2Evaluation Criteria

To facilitate direct and systematic comparison of various control strategies, a set of normalized evaluation criteria is defined in the benchmark problem definition paper. The evaluation criteria consider the ability of the controller to reduce the peak responses, the normalized responses over the entire time record, and the control requirements. Smaller values of criteria indicate superior performance. The control resource evaluation criteria are non-dimensionalised. Since the earthquake is bidirectional, the criteria are evaluated in both horizontal directions. For each control design, the evaluation criteria are found for the six specified earthquake records. The evaluation criteria are : peak base shear force (J_1), peak overturning moment (J_2), peak displacement at mid-span (J_3), peak acceleration at mid-span (J_4), peak deformation of bearings (J_5), peak curvature at bent column (J_6), peak dissipated energy of curvature at bent column (J_7), number of plastic connections (J_8), normed base shear force (J_9), normed overturning moment (J_{10}), normed displacement at mid-span (J_{11}), normed acceleration at mid-span (J_{12}), normed deformation of bearings (J_{13}), normed curvature at bent column (J_{14}), peak control force (J_{15}) and peak stroke of the control devices (J_{16}). Table 1 presents the evaluation criteria used for the present study.

2.3 Earthquake Ground Excitations

Earthquake ground motions are inherently random and multidimensional. As a consequence of the strong ground motions recorded during Kobe, Northridge and Turkey earthquakes, stronger design earthquakes are now controlling the seismic design of highway bridges. These earthquakes include the effects of near field pulses, fault normal motions and near field deep soil site motions. The six ground motions cover a large range of characteristics, namely, frequency content, duration, and PGA. The fault-normal component is applied along the transverse direction, while the fault-parallel component is applied simultaneously, along the longitudinal direction. Following six historical earthquake records are considered as ground excitations for the numerical simulations of seismic protective systems installed in the bridge: North Palm Springs

(1986) earthquake, TCU084 component of Chi-Chi earthquake, Taiwan (1999), El Centro component of 1940 Imperial Valley earthquake, Rinaldi component of Northridge (1994) earthquake, Bolu component of Duzce, Turkey (1999) earthquake and Nishi-Akashi component of Kobe (1995) earthquake. Since the bridge is located very close to active faults, five near-fault motions are considered along with the El Centro record.

3. Sliding Seismic Isolation Systems

Friction damping is one of the simplest ways of energy dissipation. Friction isolators have been widely used for seismic response mitigation of highway bridges. The performance of friction isolators is quite insensitive to large variations in the frequency content of ground excitations, making them very robust. This is the main advantage of friction isolators over elastomeric bearings. Furthermore, the provision of a restoring mechanism enhances their practicability. However, in case of near-fault motions, the sliding displacement may be unacceptably large and there may be some residual displacement after an earthquake. Large size isolators are required to accommodate such large displacements, and they demand for more space.

The seismic response of bridges isolated by elastomeric bearings and sliding systems is investigated by Kunde and Jangid (2006). Stochastic response of bridges, seismically isolated by the FPS, is examined by Jangid (2008). There are numerous examples of application of FPS in bridges, such as Benicia-Martinez Bridge and American River Bridge in California. In the recent years, there have been important studies on the use of friction isolators for protection of bridges from severe earthquake attacks. A sliding isolation system is a passive control device, based on the concept of sliding friction. Among the various friction isolators, the Friction Pendulum System is found to be the most attractive, due to its ease in installation and simple mechanism of restoring force by gravity action. In this isolator, the sliding and re-centering mechanisms are integrated in a single unit. The sliding surface of FPS is spherical, so that its time period of oscillation remains constant. Numerous studies have been carried out on the behavior of FPS during seismic events. The practical effectiveness of friction isolators can be enhanced by adding a suitable restoring mechanism, thereby reducing the residual displacements. Sliding isolators with curved surface are effective base isolation systems, incorporating isolation, energy dissipation and restoring mechanism in a single unit. In friction-type seismic isolators, isolation is achieved through sliding while energy is dissipated through sliding friction. FPS needs to be designed for a specific intensity of earthquake ground excitation. This is primarily because the maximum intensity of excitation has a strong influence on the design of FPS, even though the performance of a structure isolated with FPS is relatively independent of the frequency content of ground motion. Hence, the FPS designed for a particular intensity of excitation may not give satisfactory performance during earthquakes of lower or higher intensity.

3.1 Friction Pendulum System (FPS)

Among various friction base isolators, FPS is the most attractive due to its ease in installation and simple mechanism of restoring force by gravity action. The sliding surface of FPS is spherical so that its time period of oscillation remains constant (Zayas et al., 1990). A continuous model of frictional force of a sliding system presented by Constantinou et al. (1990) is used for the present study. The frictional forces mobilized in the sliding system are expressed by (4),

$$\mathrm{F_x} = \mathrm{F_s Z_x} \text{ and } F_y = F_s Z_y \tag{4}$$

where F_s is the limiting frictional force expressed by (5),

$$F_s = \mu\, m_d g \tag{5}$$

In Equation (5), μ is the friction coefficient of the FPS; m_d is the deck mass supported by the FPS; and *g* is the acceleration due to gravity. The dimensionless hysteretic displacement components Z_x and Z_y, represent non-linear behavior of frictional forces. The restoring force of the FPS is considered as linear (i.e. proportional to relative displacement) and is expressed by (6),

$$F_\mathrm{b} = k_\mathrm{b} x_\mathrm{b} + F_x \tag{6}$$

where F_x is the frictional force in the FPS in *x*-direction; and k_b is the stiffness of the FPS provided by the curvature of the spherical surface through inward gravity action. The FPS is designed in such a way as to provide the specific value of the isolation period, T_b expressed as (7),

$$T_b = 2\pi\sqrt{\frac{m_d}{\sum k_b}} \tag{7}$$

where $\sum k_b$ is the total horizontal stiffness of the FPS provided by its curved surface. Thus, the modeling of FPS requires the specification of two parameters, namely the isolation period (T_b) and the friction coefficient (μ).Figure 3 shows mathematical model of Friction Pendulum System.

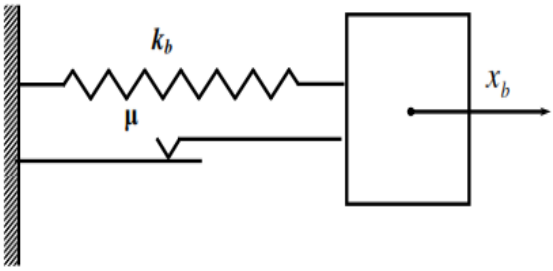

Fig. 3: Mathematical model of FPS

4. Numerical Study

The seismic response of benchmark Highway Bridge using FPSis investigated for the six specified earthquake ground excitations. To control the response, at each junction of deck and abutment, eight isolators of 1000kN capacity each are installed. All isolators contribute equally in carrying the deck-mass. The critical response quantities of interest are the base shear in piers, mid-span deck displacement and relative displacement of the isolators at the abutments. Pier base shear is directly proportional to the forces exerted in the bridge system due to earthquake ground motion. On the other hand, the relative displacement of the isolators is crucial from the design point of view of isolator and expansion joints. Optimum selection of the isolator parameters largely governs the response of the bridge. The analytical parametric study performed on FPS (μ = 0.1 and T_b = 2.5 s), proves that it performs efficiently for seismic response reduction of the benchmark highway bridge. Table 2 presents evaluation criteria with FPS. Except for peak midspan acceleration, there is substantial reduction in all response quantities. FPS is particularly found influential in controlling displacement.

Figure 4 shows ideal force-deformation behavior of sliding isolators and Figure 5 shows the hysteresis loops, when FPS is employed for the benchmark highway bridge, considering the Chi-Chi (1999) earthquake ground motion. Loops in the longitudinal as well as transverse direction are presented to show that the isolators work well in both directions. It is observed that the loops match exactly with the ideal loops presented in Figure 4. Numbers in bracket indicate maximum control force and isolator displacement.

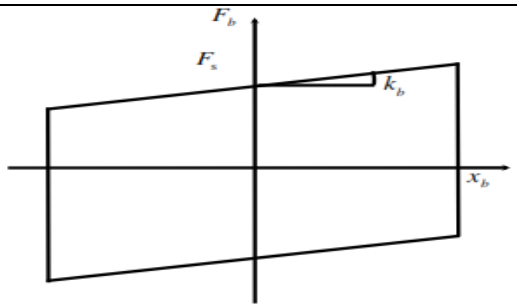

Fig. 4: Ideal force deformation behavior of FPS

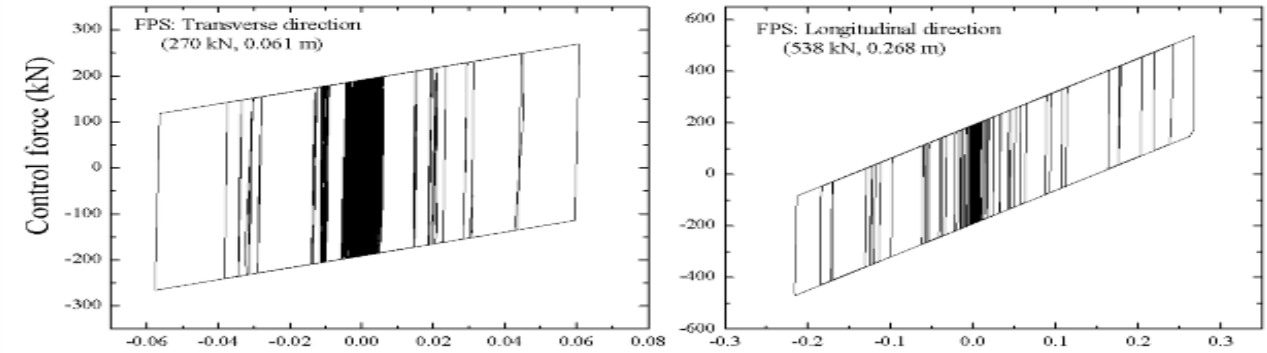

Fig.5: Force-deformation loops for FPS under Chi-Chi (1999) Earthquake ground motion

5. Conclusion

The performance of the bridge with FPS is investigated using the hysteretic model, under two horizontal components of the six earthquake excitations. The response of the bridge is evaluated using standard numerical technique and the developed SIMULINK models. The results of the numerical simulations clearly show the advantage of using sliding isolators for earthquake response mitigation of the benchmark highway bridge. Based on the investigations performed, following conclusions are drawn. (i) The optimum parameters for FPS based on the criterion of minimization of base shear and displacements of the benchmark highway bridge are μ = 0.1 and T_b =2.5s. (ii) For a low value of the friction coefficient, there is significant displacement in the FPS under near-fault motions. The increase in friction coefficient reduces thebearing displacement considerably, without much alteration to the pier base shear. (iii)The FPS is found to significantly control the peak displacement response of the deck and abutment bearings, while simultaneously limiting the pier base shear response.

REFERENCES

[1] Agrawal, A., and Tan, P. (2009). "Benchmark structural control problem for a seismically excited highway bridge-Part II: Phase I Sample control designs", *Structural Control and Health Monitoring*, 16, 2009,530-548.

[2] Constantinou, M. C., Mokha, A. S., and Reinhorn, A. M. "Teflon bearings in base isolation II: modeling", *Journal of Structural Engineering* (ASCE), 116, 1990, 455-474.

[3] Jangid, R. S. "Stochastic response of bridges seismically isolated by friction pendulum system", *Journal of Bridge Engineering*, ASCE, 13, 2008,319-330.

[4] Kunde, M. C., and Jangid, R. S. "Effects of pier and deck flexibility on the seismic response of isolated bridges", *Journal of Bridge Engineering*, ASCE, 11(1),2006,109-121.

[5] SIMULINK, The Math Works Inc., 1997, Natick, Massachusetts.

[6] Zayas, V. A., Low, S. S., and Mahin, S. A. "A simple pendulum technique for achieving seismic isolation", *Earthquake Spectra*, 6(2),1990, 317 333.

TABLE 1 Summary of Evaluation Criteria

Responses	Normed Responses	Control Strategy
Peak Base Shear $J_1 = \max\left\{\frac{\max_{i,t}\lvert F_{bi}(t)\rvert}{F_{0b}^{\max}}\right\}$	Base Shear $J_9 = \max\left\{\frac{\max_{t}\lVert F_{bi}(t)\rVert}{\lVert F_{0b}^{\max}\rVert}\right\}$	Ductility $J_6 = \max\left\{\max_{j,t}\frac{\Phi_j(t)}{\Phi^{\max}}\right\}$
Peak Overturning Moment $J_2 = \max\left\{\frac{\max_{i,t}\lvert M_{bi}(t)\rvert}{M_{0b}^{\max}}\right\}$	Overturning Moment $J_{10} = \max\left\{\frac{\max_{t,i}\lVert M_{bi}(t)\rVert}{\lVert M_{0b}^{\max}\rVert}\right\}$	Dissipated Energy $J_7 = \max\left\{\frac{\max_{j,t}\int dE_j}{E^{\max}}\right\}$
Displacement at Midspan $J_3 = \max\left\{\max_{i,t}\left\lvert\frac{y_{mi}(t)}{y_{0m}^{\max}}\right\rvert\right\}$	Displacement at Midspan $J_{11} = \max\left\{\max_{i}\frac{\lVert y_{mi}(t)\rVert}{\lVert y_{0m}^{\max}\rVert}\right\}$	Plastic Connections $J_8 = \max\left\{\frac{N_d^c}{N_d}\right\}$
Acceleration at Midspan $J_4 = \max\left\{\max_{i,t}\left\lvert\frac{\ddot{y}_{mi}(t)}{\ddot{y}_{0m}^{\max}}\right\rvert\right\}$	Acceleration at Midspan $J_{12} = \max\left\{\max_{i}\left\lVert\frac{\ddot{y}_{mi}(t)}{\ddot{y}_{0m}^{\max}}\right\rVert\right\}$	Peak force $J_{15} = \max\left\{\max_{l,t}\left(\frac{f_l(t)}{W}\right)\right\}$
Bearing Deformation $J_5 = \max\left\{\max_{i,t}\left\lvert\frac{y_{bi}(t)}{y_{0b}^{\max}}\right\rvert\right\}$	Displacement at Abutment $J_{13} = \max\left\{\max_{i}\left\lVert\frac{y_{bi}(t)}{y_{0b}^{\max}}\right\rVert\right\}$	Device Stroke $J_{16} = \max\left\{\max_{l,t}\left(\frac{d_l(t)}{x_{0m}^{\max}}\right)\right\}$

TABLE 2 Evaluation Criteria with FPS

Response Quantity / Earthquake	N Palm Springs	Chi-Chi	El Centro	Northridge	Turkey	Kobe
Peak Base Shear, J_1	1.059	0.822	0.755	0.891	0.940	0.885
Peak Base Moment, J_2	0.728	0.981	0.720	0.978	0.990	0.668
Peak Mid-span displacement, J_3	0.761	0.939	0.798	0.865	0.847	0.753
Peak Mid-span acceleration, J_4	1.147	1.044	1.049	0.996	1.000	1.039
Peak Bearing displacement,J_5	0.647	0.898	0.436	0.834	0.800	0.428
Norm Base Shear, J_9	0.944	0.860	0.554	0.811	0.855	0.717
Norm Mid-span displacement, J_{11}	0.692	0.821	0.436	0.807	0.659	0.656
Norm bearing displacement, J_{13}	0.531	0.794	0.272	0.780	0.476	0.257